Journal of Ceramic Processing Research. Vol. 21, No. 4, pp. 433~441 (2020)
(Received 21 January 2020, Received in revised form 4 April 2020, Accepted 7 April 2020)
https://doi.org/10.36410/jcpr.2020.21.4.433

J O U R N A L O F
Ceramic Processing Research

Effects of alloy ratio and coating thickness on temperature distribution of thermal barrier coatings

Can Ozturk[a] and Tolga Demircan[b,*]
[a]*Department of Mechanical Engineering, Faculty of Engineering, Kırıkkale University, Kırıkkale, Turkey*
[b]*Department of Mechanical Engineering, Faculty of Engineering, Kırıkkale University, Kırıkkale, Turkey*

Pistons on internal combustion engines that are constantly subjected to high pressure and temperature should be light, resistant to heat, resistant to corrosion and have adequate hardness to work more efficiently and to have longer lifecycles. For this purpose, piston surfaces are coated with thermal barrier that increases resistance against heat and corrosion. In this study, temperature distribution on piston surfaces were numerically analysed for ceramic coating on a piston. For this purpose, it is assumed that 100 μm NiCrAl coating is applied as bond coat on piston upper surface. This coating was coated with $MgZrO_3$+NiCrAl alloy with different alloy ratios for different coating thicknesses. $MgZrO_3$+NiCrAl alloy thickness was changed between 200 μm and 600 μm. For all analysed coating thicknesses, $MgZrO_3$ ratio in the alloy was changed between 100 to 10% and simulations were repeated for different alloy rates. As a result of these analysis, it was determined that as $MgZrO_3$ ratio in the alloy decreased, piston upper surface temperature decreased as well. For all alloy ratios, maximum temperature was observed on piston upper surface. Additionally, it was determined that as piston upper surface coating thickness increased, piston upper surface temperature increased as well.

Keywords: Functional ceramic coating, Thermal barrier coating, Coating thickness, Coating alloy ratio.

Introduction

As ceramic materials have high resistance, and can conduct heat and electricity at high levels, this material is commonly used in engineering applications to increase efficiency and durability. One of these materials is known as zirconium dioxide. ZrO_2 is used in aviation industry, gas turbines, and certain engine components. In this study, the purpose was to apply Magnesium ZrO_3, which is a zirconium-based ceramic on piston surface in graded way. The purpose of using different functional graded materials on a piston is to increase piston resistance, enable upper surface of piston to achieve higher temperatures, thus, increase overall efficiency. For this purpose, in this study, different coating ratios and thickness with $MgZrO_3$ (Magnesium zirconium oxide) and connection layer that will be applied on the upper surface of a designed diesel engine piston was calculated numerically. After the analysis, maximum and minimum temperature changes were obtained for diesel engine piston. Some of the studies in the literature regarding piston ceramic coating were given below.

Cerit and Çoban [1] numerically analysed thermal properties of an aluminium alloy piston coated with ceramic in a diesel engine. Authors compared temperature values for coated and uncoated piston by using finite element analysis. Authors stated that temperature values of coated piston surface was higher than uncoated piston surface. Büyükkaya [2] analysed thermal behaviours of functional graded aluminium-silicon alloy piston and steel pistons with package program. Author compared temperature values of piston coated with AlSi allow and uncoated piston. As a result, author found that piston surface value of FGM coated AlSi piston was 28% higher than uncoated piston surface temperature. It was observed that surface temperature of steel piston increased 17%. Büyükkaya and Cerit [3] conducted numerical 3 dimensional thermal analysis on ceramic coated diesel engine piston. MgO, ZrO, and AlSi alloy coated pistons and uncoated pistons were simulated. It was observed that maximum surface temperature of steel piston was higher than AlSi alloy piston.

Gehlot and Tripathi [4] evaluated thermal analysis of holes that are created to coat ceramic to the piston of a diesel engine. Analysis were conducted for piston geometries with 1.5 mm, 2 mm, and 2.5 mm radius holes. Authors observed that as radius of holes increased, temperature of upper surface (coated surface) increased, and when coats had holes, upper surface temperature levels of piston significantly increased. Cerit et al. [5] analysed effect of partially ceramic coated piston use in spark ignition engine on HC emission. For engine tests, both standard piston and coated piston was selected. Authors observed that with coating, surface temperature

*Corresponding author:
Tel : +90 3183574242 / 1057
Fax: +90 3183572459
E-mail: tolgademircan@gmail.com

of piston increased up to 100 °C. Robinson and Palaninathan [6] conducted thermal analysis for piston cast by using three dimensional finite element method. Authors determined that the thinnest part solidifies in one second while middle part solidifies after sixty seconds. Kummitha and Reddy [7] numerically analysed thermal effect of using different materials on winged cylinder block. Authors determined that heat transfer speed of the material was linked with thermal conductivity of material.

Dudareva et al. [8] analysed microarc oxidation (MAO) coating application for thermal protection of internal combustion engine piston upper surface. Tests were conducted for 76 and 106 μm MAO coating thicknesses and it was determined that piston temperatures decreased by 45 and 78 °C respectively. Dhinest et al. [9] numerically and experimentally analysed thermal properties of coated diesel engine that works with nano biofuel. For this purpose, engine piston, valves and cylinder head was coated with YSZ (Yttria-stabilised zirconia) coating. As a result, it was determined that average temperatures of these components increased, harmful emission decreased and engine thermal efficiency increased by 1.75% compared to conventional engines. Yao et al. [10] analysed effects of thermal barrier coating on a diesel engine on combustion and resulting emissions. For this purpose, simulations are conducted for two different engine loads (6 bar IMEP and 17.9 bar IMEP). Results of their study showed that thermal barrier applications have the ability to decrease thermal transfer losses on piston walls and this might increase engine thermal efficiency. Lu et al. [11] analysed effects of diesel engine YSZ thermal barrier coating application on thermal behaviour. Authors reported that coating application significantly affected piston peak temperature distribution. It was observed that as coating thickness increased, piston upper surface temperature increased and coating and piston mid-surface temperature decreased. Authors stated that this might lead lower thermal loss in combustion chamber and increased thermal efficiency.

Muthusamy et al. [12] experimentally analysed effect of engine piston thermal barrier coating (8YSZ-TiO_2-Al_2O_3) application on engine efficiency and resulting emissions. For same operating conditions, it was observed that thermal efficiency increased 5.99% for thermal barrier coating practice compared to uncoated condition. On the other hand, specific fuel consumption decreased by 0.06 kg/kWh. It was also noted that combustion caused HC and CO emission decreased as well. Cerit [13] analysed effects of coating thickness and size of a ceramic coated internal combustion engine piston on temperature and stress distribution. As coating thickness increased, it was observed that coating surface temperature increased as well. With increasing coating thickness, it was noted that normal stress on piston surface decreased and shear stress slightly increased. For analysed coating thickness, optimal coating thickness value was identified as 1 mm. Sachit et al. [14] numerically analysed thermal effects of Cr_2O_3 coating on diesel engine piston upper surface. Their study showed that Cr_2O_3 coating on piston surface increased surface temperature compared to uncoated condition.

Yao and Qian [15] investigated effects of nano-ceramic coated piston use in natural gas engine on piston temperature distribution. Authors compared these results with uncoated piston. For those parameters, piston upper surface temperature of coated piston had approximately 44% higher average temperature than uncoated piston and piston coating bottom average temperature decreased approximately 12%. Mahade et al. [16] analysed effects of YSZ coating thickness in gadolinium zirconate/YSZ couple on resistance. To determine thermal conductivity and thermal shock lifecycle of Thermal Barrier Coating, experiments were conducted for different gadolinium zirconate (GZ) and YSZ thicknesses. Minimum thermal conductivity was observed for thinnest YSZ coating. Additionally, it was reported that as YSZ thickness increased, thermal shock lifecycle decreased. Garud et al. [17] analysed effects of a diesel engine piston surface thermal barrier coating (YSZ) application on engine performance and combustion properties. For this purpose, piston upper surface was coated with 250 micron thick YSZ (Y_2O_3 & ZrO_2) ceramic material with plasma spraying technique. As a result, it was observed that piston upper surface YSZ thermal barrier coating increased engine break thermal efficiency by 1.4% compared to uncoated condition.

Yao et al. [18] experimentally and numerically analysed Nano PYSZ Thermal Barrier Coating on temperature and thermal load distribution. For this purpose, aluminium allow piston surfaces were coated with Nano PYSZ thermal barrier. As a result, it was observed that Nano PYSZ coated piston lower layer temperatures decreased by 16% compared to uncoated piston. It was determined that piston upper surface temperature approximately increased 52%. Authors reported that this could increase engine combustion chamber temperature and engine efficiency. Venkadesan and Muthusamy [19] experimentally analysed Al_2O_3/8YSZ and CeO_2/8YSZ alloy coating of diesel engine piston surfaces on engine performance and emission properties. For this purpose, aluminium piston upper surface was first coated with CoNiCrAlY bonding layer. These layers were coated with two different coating material as 20%Al2O3/80%8YSZ and 20%CeO2/80%8YSZ and experiments were conducted. Results showed that CeO_2/8YSZ based coating had better thermal cycle behaviour compared to Al_2O_3/8YSZ based coating. For both thermal coating material, it was reported that break thermal efficiency increased and fuel consumption decreased for uncoated condition. Additionally, it was reported that HC, CO and smoke decreased and NOx

emission increased.

Moon et al. [20] investigated the effects of plasma spraying ZrO_2 based thermal barrier coating on the phase change for different thermal cycles. For this purpose, ZrO_2-$8Y_2O_3$ and ZrO_2-25CeO2-$2.5Y_2O_3$ materials were subjected to heat treatment at 1300 ºC and 1500 ºC for 100 hours and cooled down with 4 different cooling methods. As a result, it was found that the amount of oxygen gap was the main factor for phase change behaviour and had a strong correlation with cooling ratio. Lee et al. [21] studies on the effect of coating thickness of thermal barrier coatings (TBCs) on contact fatigue and abrasion behaviour. Bond coat material thickness was kept constant at 250 μm and thermal barrier coating (TBC) material thickness was changed as 200, 400 and 600 μm. As a result, it was found that TBC coating thickness change had a significant effect on the mechanical behaviour of gas turbine operation. Cho et al. [22] gas turbine were coated with yttrium stabilized zirconia (YSZ) and thermal and mechanical behaviours of the coated thermal barriers were investigated. NiCrCoAlY was used as the binder. Thermal barrier layer thermal resistance was determined with thermal annealing and hardness measurements. As a result, it was observed that pre-heat treated thermal barrier coating offered advantages in thermal and mechanical resistance.

Lee et al. [23] analysed nano-structured SiC reinforced zirconia-based thermal barrier coatings. For this purpose, ZrO_2-$25CeO_2$-$2.5Y_2O_3$ (CYSZ) coatings were investigated. As a result, it was determined that the friction coefficient decreased with SiC reinforcement. Kim et al. [24] analysed residual stresses and thermal conductivity values of 3YSZ/LaPO composite thermal barrier coating (TBC) prepared by atmospheric plasma spraying method. It was determined that the thermal conductivity of the coating layers had lower values than sintered materials. Yao ve Li [25] applied thermal barrier coating to an aluminium alloy piston with PYSZ (TBC Nano yttria partially stabilized zirconia) material and investigated the piston microstructure and thermal behaviour. As a result, when the ceramic coating thickness was increased from 0,1 mm to 1.4, TBC applied piston maximum temperature increased from 399 ºC to 665 ºC. It was determined that aluminium alloy sub-layer maximum temperature decreased from 336 ºC to 241 ºC. It was observed that thermal insulation performance increased as the ceramic layer thickness increased. Caputo et al. [26] experimentally and numerically investigated the effects of a thermal barrier coating on a diesel engine piston on fuel consumption and emission. The results of the study showed that when TBC is applied to the pistons, fuel consumption decreased approximately by 1% and thermal transfer decreased by 6%. However, due to increased surface graining, a relative decrease in engine efficiency was determined.

Reghu et al. [27] numerically and experimentally investigated the effects of 8YPSZ coating on Al-Si alloy on the thermal barrier. For different layer thicknesses, temperature decrease was determined along the upper surface and lower layers of the thermal barrier coating. In this experiment, for coating thickness of 100 mm, 250 mm and 500 mm, maximum 57 ºC, 170 ºC and 248 ºC temperature decrease were observed. Numerical analysis was conducted for the same parameters and it was reported that the obtained results are in line with the experimental results. Ramaswamy et al. [28] developed a model to predict the effects of thermal barrier coating (TBC) thickness inconsistencies applied to internal combustion engine pistons. The results obtained from this model were verified with the experimental study and it was determined that this model was reliable. Yerrennagoudaru and Manjunatha [29] conducted a numerical combustion analysis for platinum coated and uncoated states of a piston modified from a diesel engine. The results showed that the thermal stress of the modified piston was lower than the conventional piston. The upper surface temperature of the platinum coated piston was observed to have a higher temperature vale than the uncoated piston. It is stated that coating the piston with platinum might help combusting fuels with lower Centene value.

In this study, temperature distribution on piston surfaces were numerically analysed with Ansys package program for ceramic thermal barrier coating on diesel engine piston. Material of diesel engine was selected as aluminium silicon. Piston coating was selected as NiCrAl alloy. Additionally, $MgZrO_3$+NiCrAl alloy was applied to the upper surface of the piston as functional graded material. Based on change of functional graded coating rates and thicknesses, analysis were conducted and changes in piston temperature distribution were evaluated.

Definition of Problem and Mathematical Formulation

In this study, temperature distribution on piston surfaces were numerically analysed for ceramic coating on diesel engine piston. Adopted piston geometry was presented in Fig. 1. As seen from the figure, piston evaluated in this study had diameter of D = 130 mm, and piston length of H = 147.76 mm. 100 micrometre thick NiCrAl coating was applied as bond coat on the upper surface of the piston. On this coating, graded $MgZrO_3$+NiCrAl alloy with 200, 300, 400, 500 and 600 micrometre thicknesses were applied for different alloy ratios. In graded coated sections of piston, simulations were repeated for 100%, 90%, 70%, 50%, 30%, and 10% $MgZrO_3$.

Mesh Structure

Mesh structure of the piston analysed in this study

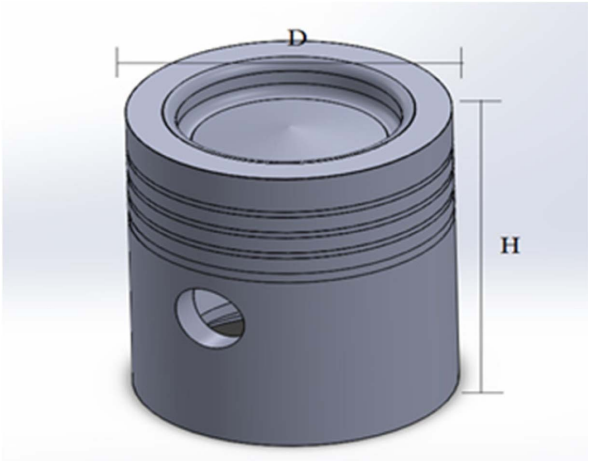

Fig. 1. Piston Geometry.

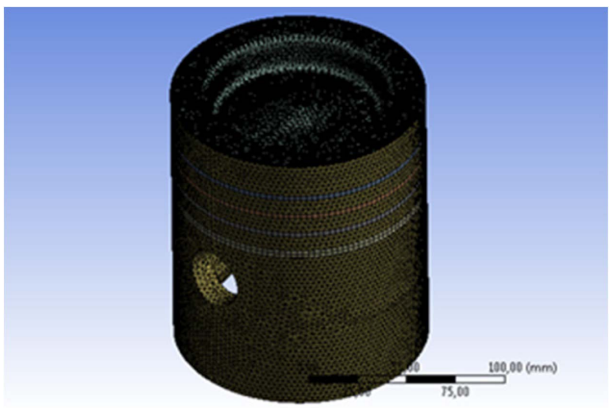

Fig. 2. Mesh structure of problem.

was presented in Fig. 2. To determine optimum mesh structure, analysis were repeated for mesh structures with different node numbers. Based on the obtained results, optimum node number was determined as about 570000, and all analysis were conducted based on optimum mesh structure.

Validation of numerical method

To determine whether numerical results are within reliable region, these results should be compared with other studies accepted as reliable. For this purpose, geometry and boundary conditions of previous studies in the literature were repeated in simulation. Obtained results and sample results from literature [4] were presented in Fig. 3.

In Fig. 3, change of surface temperature along piston side surfaces were presented for both studies. As seen from the figure, surface temperature curves for both studies are similar. Therefore, it could be said that results obtained from numerical methods employed in this study are reliable.

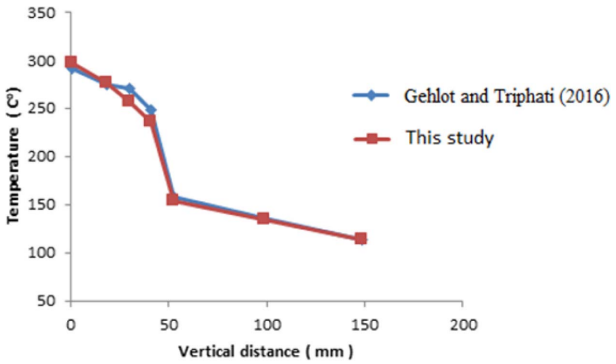

Fig. 3. Comparison of piston outer side surface temperature change with literature.

Findings and Discussion

In this study, functional graded ceramic coating applied on a designed diesel engine and temperature distribution on piston upper surface based on bond coating were numerically evaluated for maximum and minimum temperature changes on piston volume. For this purpose, upper surface of piston was coated with ceramic to have bond coat thickness of micrometre, and graded coat thickness of 100, 200, 300, 400, 500 and 600 micrometre. Graded coating was applied as $MgZrO_3$ and NiCrAl alloy. Piston bond coat was kept constant as 100 micrometre NiCrAl alloy, and on this layer, graded $MgZrO_3$ was applied with 100%, 90%, 70%, 50%, 30%, and 10% ratio, and numerical simulations were repeated for graded coating. Some of the analysis results were presented below.

Fig. 4 showed temperature distributions for graded coat thickness 300 and different $MgZrO_3$ alloy ratio. In this figure, 6 different states with 100%, 90%, 70%, 50%, 30%, and 10% $MgZrO_3$ were presented. As seen from figures, temperature distribution on pistons were similar for all states. While maximum temperature was observed on the upper surface of the piston, temperatures decreased along the piston, and had minimum value at the bottom surface.

For constant coating thickness, decreased $MgZrO_3$ alloy ratio decreased temperatures observed on all piston surfaces. Especially, piston upper surface temperature significantly decreased as $MgZrO_3$ alloy ratio decreased. Piston upper surface maximum temperature value was identified for 100% and 10% $MgZrO_3$ alloy ratio as 379.03 and 302.46 °C respectively. As alloy ratio of ceramic coating decreased, piston upper surface maximum temperature approximately decreased 20.2%. For 6 different alloy ratio, piston bottom surface temperature was approximately 113 °C. Therefore, piston bottom surface temperature was not significantly affected from $MgZrO_3$ alloy ratio.

For different alloy ratios, graphics that show radial piston upper surface temperature change were plotted

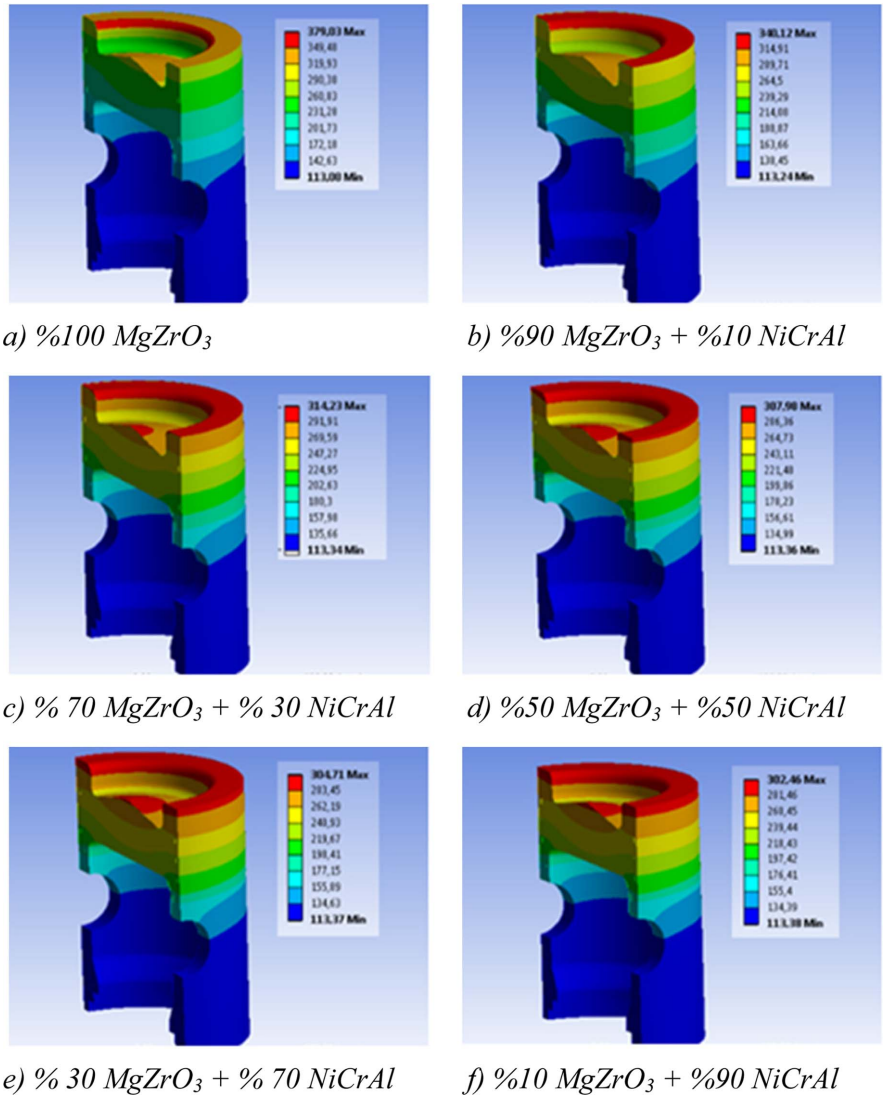

Fig. 4. Temperature distributions for a piston with different graded $MgZrO_3$ coating ratios a) 100%, b) 90%, c) 70%, d) 50%, e) 30%, f) 10%.

for 200, 300, 500 and 600 µm coating thickness. These graphs are presented in Fig. 5. These figures show radial piston upper surface temperature change along piston diameter. For constant coating thickness, curves plotted for all alloy ratios had similar structure. All curves present a symmetrical structure compared to piston centre. Temperature level slightly changes for first 20 mm distance from piston outer surface to centre. From this distance, temperature values suddenly decrease and reach minimum level. Temperature values increase around piston centre. At the central point of the piston, temperature levels reach maximum level. This is similar for all analysed alloy ratio and coating thicknesses.

As seen from this figure, for all coating thicknesses, piston upper surface temperatures are at maximum level when alloy ratio was 100%. With decreases alloy ratio, piston upper surface temperature decreased as well. When alloy ratio was 90%, piston upper surface temperatures decreased. When alloy ratio was between 70-10%, temperatures obtained for these ratios had similar structure. For four coating thickness in the figure, there is similar structure. Therefore, for constant coating thickness, as ceramic coating $MgZrO_3$ alloy ratio increased, it can be stated that piston upper surface temperature value increased. Especially when $MgZrO_3$ ratio in coating was 70% or higher, these ratios have significant effect on piston upper surface temperature distribution. Additionally, curves for alloy ratio of 70% of lower were slightly effected from coating thickness increase. Temperatures are at similar level. However, temperature values for alloy rate of 70% or higher increases as coating thickness increases. These values reach maximum value for coating thickness of 600 µm. Therefore, with increasing coating thickness, temperature difference between 70% and 100% alloy curves increase.

For different coating thickness, graphics that show

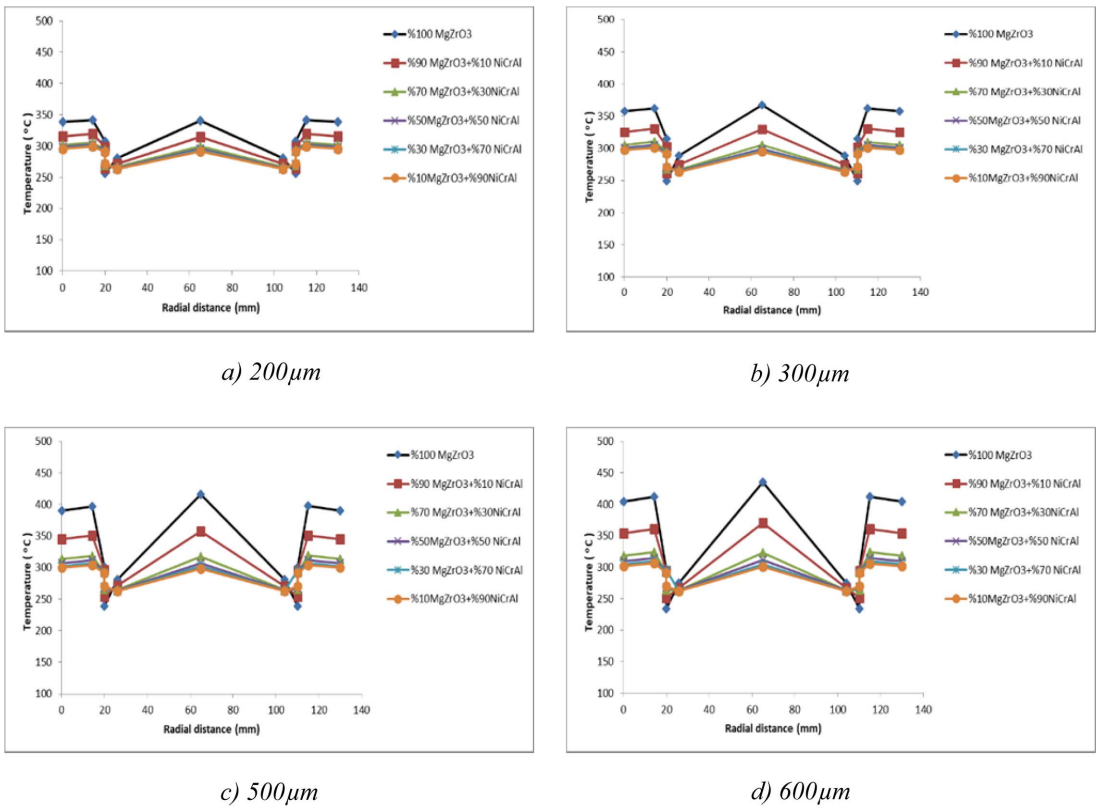

a) 200µm *b) 300µm*

c) 500µm *d) 600µm*

Fig. 5. Radial change of piston upper surface temperature for different $MgZrO_3$ ratio a) 200 µm, b) 300 µm, c) 500 µm, d) 600 µm.

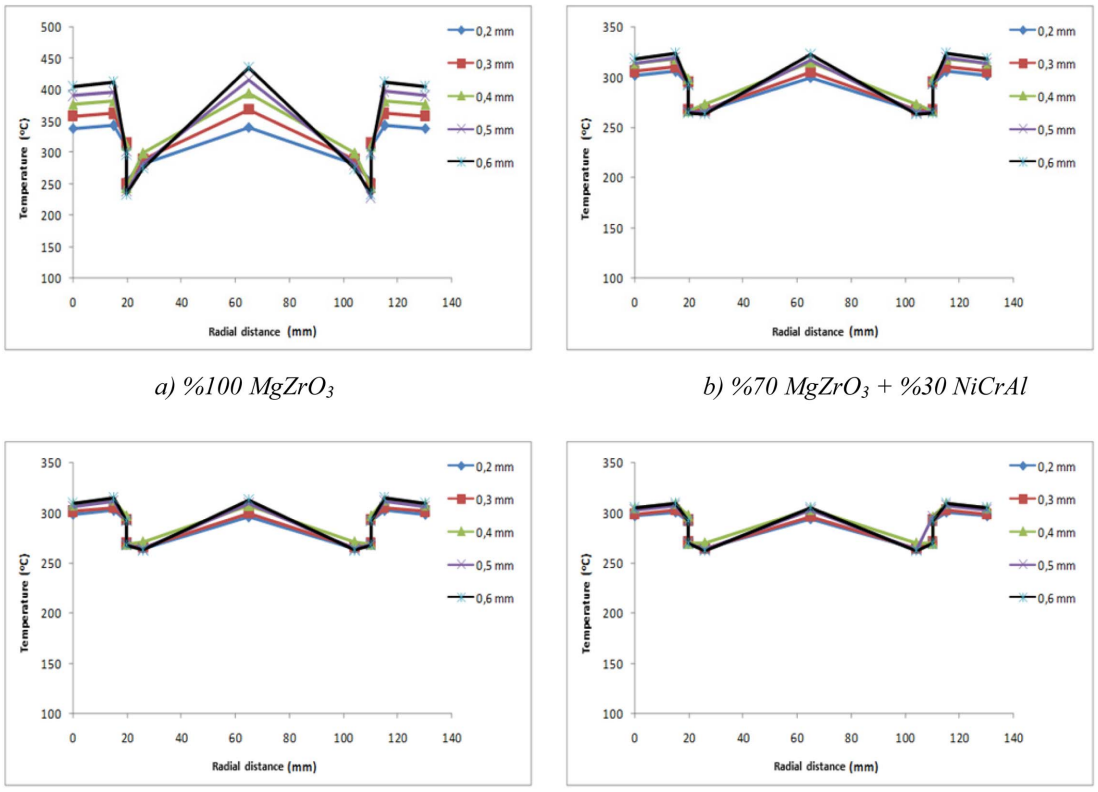

a) %100 $MgZrO_3$ *b) %70 $MgZrO_3$ + %30 NiCrAl*

c) % 50 $MgZrO_3$ + % 50 NiCrAl *d) %30 $MgZrO_3$ + %70 NiCrAl*

Fig. 6. Radial change of piston upper surface temperature for different coating thickness a) %100 $MgZrO_3$, b) %70 $MgZrO_3$, c) %50 $MgZrO_3$, d) %30 $MgZrO_3$.

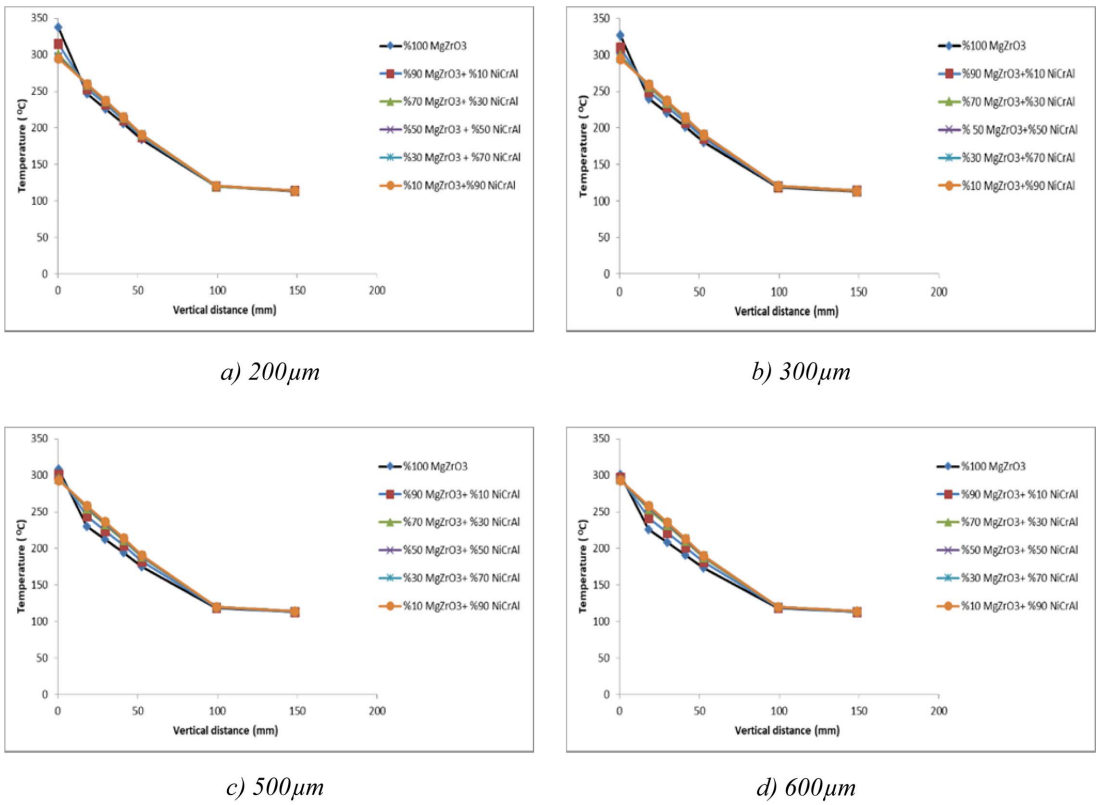

Fig. 7. Temperature change along outer edge vertical length of piston for different alloy ratios a) 200 μm, b) 300 μm, c) 500 μm, d) 600 μm.

radial piston upper surface temperature change were plotted for 100%, 70%, 50% and 30% ceramic coating alloy ratio. These graphs are presented in Fig. 6. These figures show radial piston upper surface tem- perature change along piston diameter. For constant coating thickness, curves plotted for all alloy ratios had similar structure. All curves present a symmetrical structure compared to piston centre. As seen from the figure, for constant alloy rates, increased coating thickness increases piston upper surface temperature. Especially when coating alloy ratio was 100% $MgZrO_3$, increased coating thickness can significantly increase piston upper surface temperature. With decreasing alloy ratio, effect of coating thickness on temperature distribution decreases as well. Small alloy ratios has similar temperature curves for all analysed coating thicknesses.

In Fig. 7, piston upper surface temperature changes for different alloy rates are presented for 200 μm, 300 μm, 500 μm and 600 μm coating thickness. These figures show piston outer surface temperature change from piston upper surface to piston bottom surface along vertical axis. When this figure was analysed, for all alloy ratios, upper surface of the piston showed maximum temperature, and temperatures decreased along the piston to minimum level. Maximum temperature on the upper surface of the piston was observed in 100% $MgZrO_3$ alloy model. With decreased $MgZrO_3$ alloy ratio, piston upper temperature decreased as well. However, this changed approximately 15mm after the upper part of the piston and reverse states were observed. While maximum temperature in that region was observed for 10% $MgZrO_3$ alloy, temperatures decreased with increased alloy ratio. Especially with increasing coating thickness, temperature values observed in this region are effected from coating alloy rate changes. 100 mm after the upper part of the piston, alloy ratio on the piston had almost no significant effect on temperature change, and all curves have similar structure in piston skirt. This is similar for all analysed coating thicknesses.

In Fig. 8, piston central axis temperature changes for different alloy rates are presented for 200 μm, 300 μm, 500 μm and 600 μm coating thickness. These figures show piston central axis temperature change from piston upper surface to piston bottom surface along vertical axis. When this figure was analysed, for all alloy ratios, upper surface centre of the piston showed maximum temperature, and temperatures decreased along piston central axis and reached minimum level. For piston upper surface centre, maximum temperature was observed for 100% $MgZrO_3$ alloy coating model and minimum temperature was observed for 10% $MgZrO_3$ alloy coating model. $MgZrO_3$ alloy ratio decreased, piston upper central temperature decreased as well. However, this changed approximately 10-15 mm after the upper part of the piston and reverse states

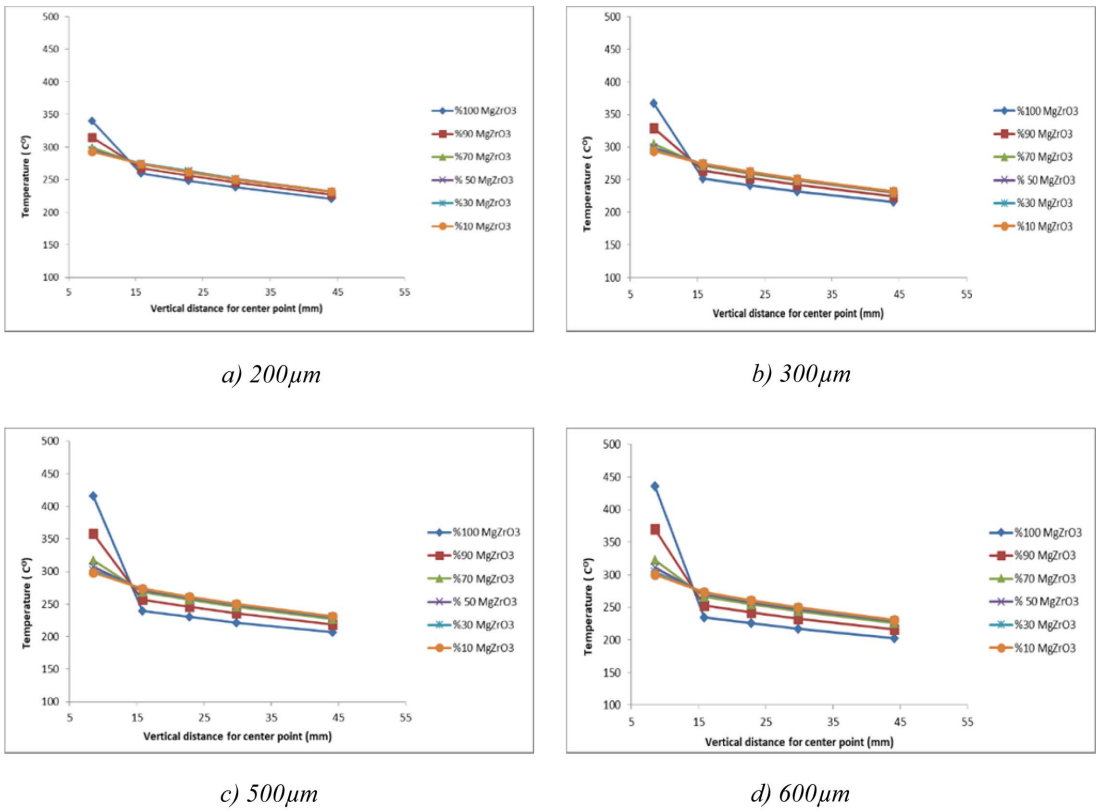

a) 200µm *b) 300µm*

c) 500µm *d) 600µm*

Fig. 8. Temperature change of piston central axis along with vertical length for different alloy ratios a) 200 µm, b) 300 µm, c) 500 µm, d) 600 µm.

were observed. From this point, temperature decreases with increasing alloy rate. While maximum temperature was observed for 10% $MgZrO_3$, minimum temperature was observed for 100% $MgZrO_3$. This case was similar along piston central axis. For all analysed coating thicknesses, temperature curves show similar structure. Additionally, for 200 µm coating thickness, temperature curves for different alloy rates have similar levels. However, these curves diverge with increasing coating thickness.

Results

In this study, temperature distribution on piston surfaces were numerically analysed for ceramic thermal barrier coating on diesel engine piston. 100 micrometre thick NiCrAl coating was applied as bond coat on the upper surface of the piston. On this coating, graded $MgZrO_3$+NiCrAl alloy with 100, 200, 300, 400, 500 and 600 micrometre thicknesses were applied for different alloy ratios. In graded coated sections of piston, simulations were repeated for 100%, 90%, 70%, 50%, 30%, and 10% $MgZrO_3$. As a result of the analysis, it was determined that for all alloy ratios, upper surface of the piston showed maximum temperature, and temperatures decreased along the piston to minimum level at piston skirt region. Maximum temperature on the upper surface of the piston was observed in 100% $MgZrO_3$ alloy model. $MgZrO_3$ alloy ratio decreased, piston upper temperature decreased as well. In skirt region of the piston, it was observed that alloy ratio had no significant effect on temperature values. Minimum upper surface temperatures were determined for alloy ratio between 70-10% and it was observed that these temperatures were similar. All these coating thicknesses showed similar behaviour. For constant alloy ratio, increased coating thickness also increased piston upper surface temperature. As a result, using different functional graded materials on a piston increases piston resistance, enables upper surface of piston to achieve higher temperatures, thus, increases overall thermal efficiency. Considering this factors, it could be stated that 600 µm thickness and 100% $MgZrO_3$ alloy coated piston model was the best state for analysed problem.

Note: Preliminary work of this paper are presented as abstract proceeding in Engineers of the Future International Student Symposium-EFIS2017 organised in Zonguldak, Turkey between 07-09 June 2018.

References

1. M. Cerit and M. Çoban, Int. J. Therm. Sci. 77 (2014) 11-18.
2. E. Büyükkaya, Surf. Coat. Tech. 202[16] (2008) 3856-3865.

3. E. Büyükkaya and M. Cerit, Surf. Coat. Tech. 202 (2007) 398-402.
4. R. Gehlot and B. Tripathi, J. Case Stu. Therm. Eng. 8 (2016) 291-299.
5. M. Cerit, V. Ayhan, A. Parlak, and H. Yasar, J. App. Therm. Eng. 31[2-3] (2011) 336-341.
6. D. Robinson and R. Palaninathan, Int. J. Fin. Elem. Analy. Des. 37[2] (2001) 85-95.
7. O.R. Kummitha and B.V.R. Reddy, J. Mater. T. 4[8] (2017) 8142-8148.
8. N.Y. Dudareva, R.D. Enikeev, and V.Y. Ivanov, Proc. Eng. 206 (2017) 1382-1387.
9. B. Dhinesh, Y.M.A. Raj, C. Kalaiselvan, and R. Krishna-Moorthy, Energy Conv. Man. 171 (2018) 815-824.
10. M. Yao, T. Ma, H. Wang, Z. Zheng, H. Liu, and Y. Zhang, Energy. 162 (2018) 744-752.
11. G.X. Lu, L.J. Hao, C. Liu, and F.X. Ye, Mater. Sci. Tech. 30[11] (2014) 1273-1282.
12. J. Muthusamy, G. Venkadesan, and U. Krishnavel, Therm. Sci. 20[4] (2016) S1189-S1196.
13. M. Cerit, Surf. Coat. Tech. 205[11] (2011) 3499-3505.
14. T.S. Sachit, R.V. Nandish, and Mallikarjun, Mater. T. Proc. 5[2] (2018) 5074-5081.
15. Z. Yao and Z. Qian, J. Alloy Comp. 768 (2018) 441-450.
16. S. Mahade, N. Curry, K.P. Jonnalagadda, R.L. Peng, N. Markocsan, and P. Nylén, Surf. Coat. Tech. 357 (2019) 456-465.
17. V. Garud, S. Bhoite, S. Patil, S. Ghadage, N. Gaikwad, D. Kute, and G. Sivakumar, Mater. T. Proc. 4[2] (2017) 188-194.
18. Z. Yao, K. Hu, and R. Li, J. Alloy Comp. 790 (2019) 466-479.
19. G. Venkadesan and J. Muthusamy, Cer. Int. 45[3] (2019) 3166-3176.
20. J. Moon, H. Choi, and C. Lee, J. Ceram. Process. Res. 1[1] (2000) 69-73.
21. D.H. Lee, B. Jang, C. Kim, and K.S. Lee, J. Ceram. Process. Res. 20[5] (2019) 499-504.
22. J.H. Cho, T.W. Kim, Y.G. Jung, K.D. Lee, J. Ceram. Process. Res. 10[3] (2009) 344-350.
23. J.W. Lee, C.H. Lee, H.J. Kim, J. Ceram. Process. Res. 2[3] (2001) 113-119.
24. S.H. Kim, Z.Y. Fu, K. N, and S.W. Lee, J. Ceram. Process. Res. 12[2] (2011) 126-131.
25. Z. Yao and W. Li, J. Alloy Comp. 812 (2020) 152162.
26. S. Caputo, F. Millo, G. Boccardo, A. Piano, G. Cifali, and F.C. Pesce, J. App. Therm. Eng. 162 (2019) 114233.
27. V.R. Reghu, A. Basha, K. Lobo, S. Shivakumar, P. Tilleti, V. Shankar, and P. Ramaswamy, Mater. T. Proc. 19 (2019) 630-636.
28. P. Ramaswamy, V. Shankar, V.R. Reghu, N. Mathew, and S. Manoj Kumar, Mater. T. Proc. 5 (2018) 12623-12631.
29. H. Yerrennagoudaru and K. Manjunatha, Mater. T. Proc. 4[2] (2017) 2333-2340.